Supplementary Information

Metal-organic Framework-derived Hierarchical Porous N-doped Carbon Supported Sponge-like Pd-SnO_2 Nanostructures for Low-temperature CO Oxidation

Adewale K. Ipadeola[a,b], Ahmed Gamal[a,b,c], Belal Salah[a,b], Yassmin Ibrahim[a,b], Aboubakr M. Abdullah[a*], Aderemi B. Haruna[c], Kenneth I. Ozoemena[c] and Kamel Eid[b*]

[a.]Center for Advanced Materials, Qatar University, Doha 2713, Qatar.

[b.]Gas Processing Center(GPC), College of Engineering, Qatar University, Doha 2713, Qatar.

[c.]Molecular Science Institute, School of Chemistry, University of the Witwatersrand, Private Bag 3, PO Wits, Johannesburg, South Africa

*Corresponding authors: bakr@qu.edu.qa; kenneth.ozoemena@wits.ac.za; kamel.eid@qu.edu.qa

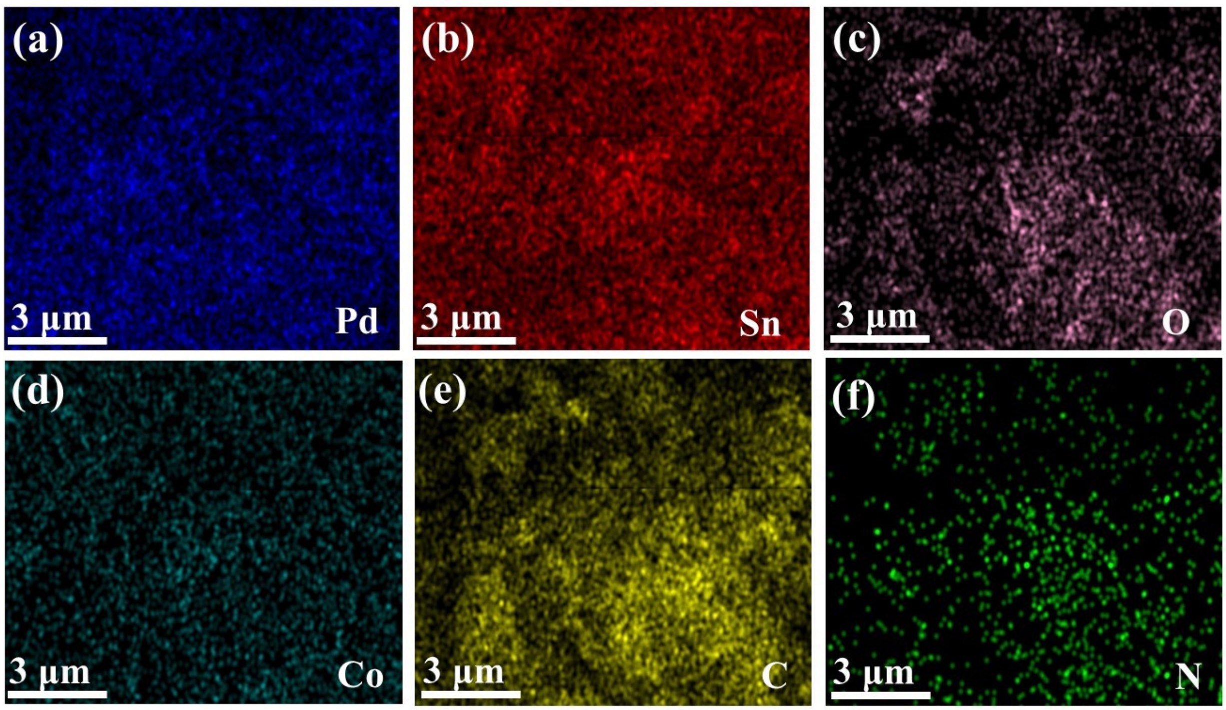

Fig. S1. Elemental mapping (a) Pd, (b) Sn, (c) O, (d) Co, (e) C and (f) N of Pd-SnO_2/MOF-PNC

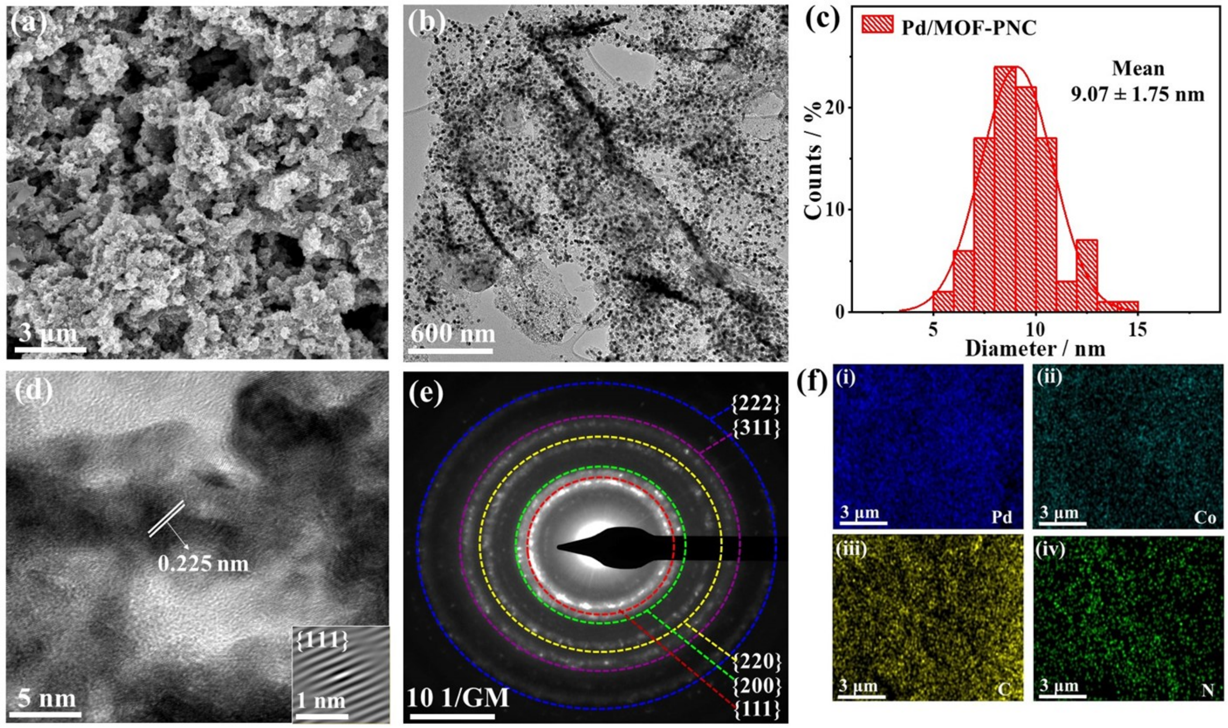

Fig. S2. (a) SEM, (b) TEM, (c) Nanoparticles size distribution, (d) HRTEM, (e) SAED, and (f) Elemental mapping (i) Pd, (ii) Co, (iii) C and (iv) N of Pd-of Pd/MOF-PNC.

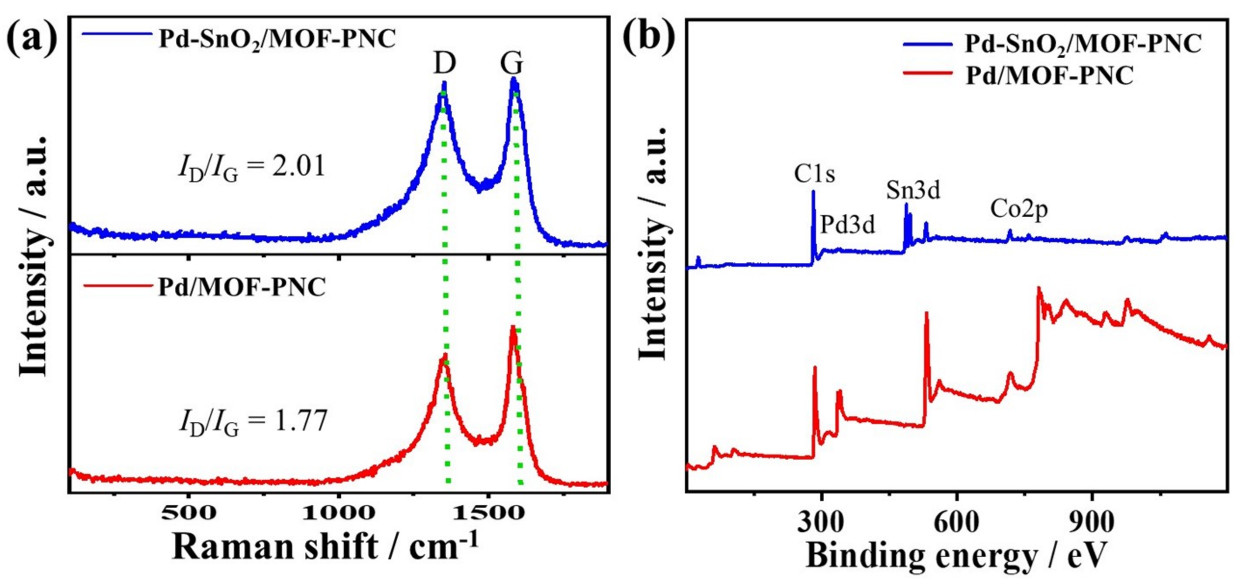

Fig. S3. (a) Raman spectra and XPS wide scans of Pd-SnO_2/MOF-PNC and Pd/MOF-PNC

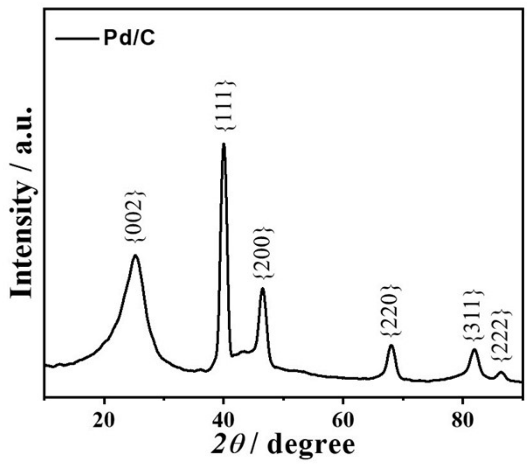

Fig. S4. XRD of Pd/C taken from the JCPDS database

Table S1. XPS and EDX atomic contents of elements in Pd-SnO_2/MOF-PNC and Pd/MOF-PNC

	XPS		EDX		ICP-OES		
	Pd-SnO_2/MOF-PNC	Pd/MOF-PNC	Pd-SnO_2/MOF-PNC	Pd/MOF-PNC	Pd-SnO_2/MOF-PNC	Pd/MOF-PNC	Pd/C
Pd	2.16 At.%	2.71 At.%	2.31 At.%	2.12 At.%	15.90 wt.%	17.70 wt.%	19.78 wt.%
Sn	3.57 At.%	-	1.31 At.%	-	18.12 wt.%	-	-
Co	4.50 At.%	15.88 At.%	2.52 At.%	5.29 At.%	3.16 wt.%	11.24 wt.%	-
C	78.86 At.%	80.97 At.%	66.21 At.%	49.81 At.%	-	-	-
O	10.42 At.%	-	11.93 At.%	23.24 At.%	-	-	-
N	0.39 At.%	0.44 At.%	15.72 At.%	20.54 At.%	-	-	-

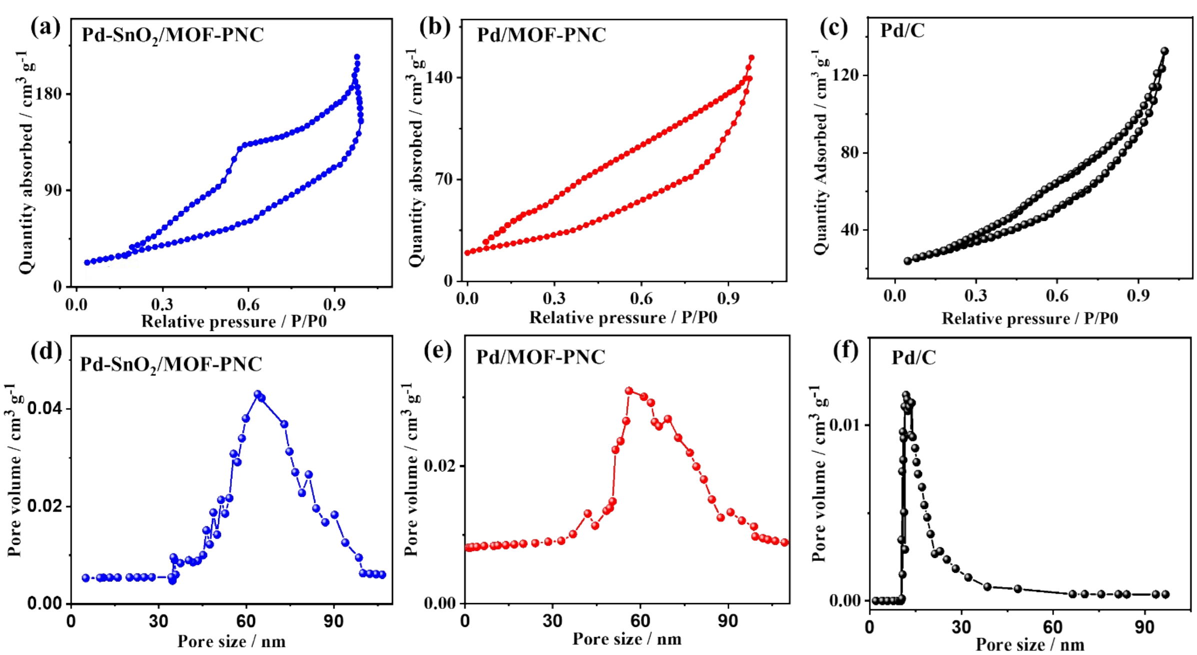

Fig. S5. (a-c) N_2-adsorption/desorption isotherm and (d-e) pore size distribution of Pd-SnO_2/MOF-PNC, Pd/MOF-PNC, and Pd/C.

Table S2: Binding energies of Pd 3d spectra of Pd-SnO_2/MOF-PNC and Pd/MOF-PNC catalysts

Catalysts	Pd $3d_{5/2}$			Pd $3d_{3/2}$		
	Pd^0	Pd^{2+}	Pd^{4+}	Pd^0	Pd^{2+}	Pd^{4+}
Pd-SnO_2/MOF-PNC	335.42	336.25	337.92	341.25	342.75	343.86
Pd/MOF-PNC	335.34	336.09	337.58	340.95	341.82	343.61

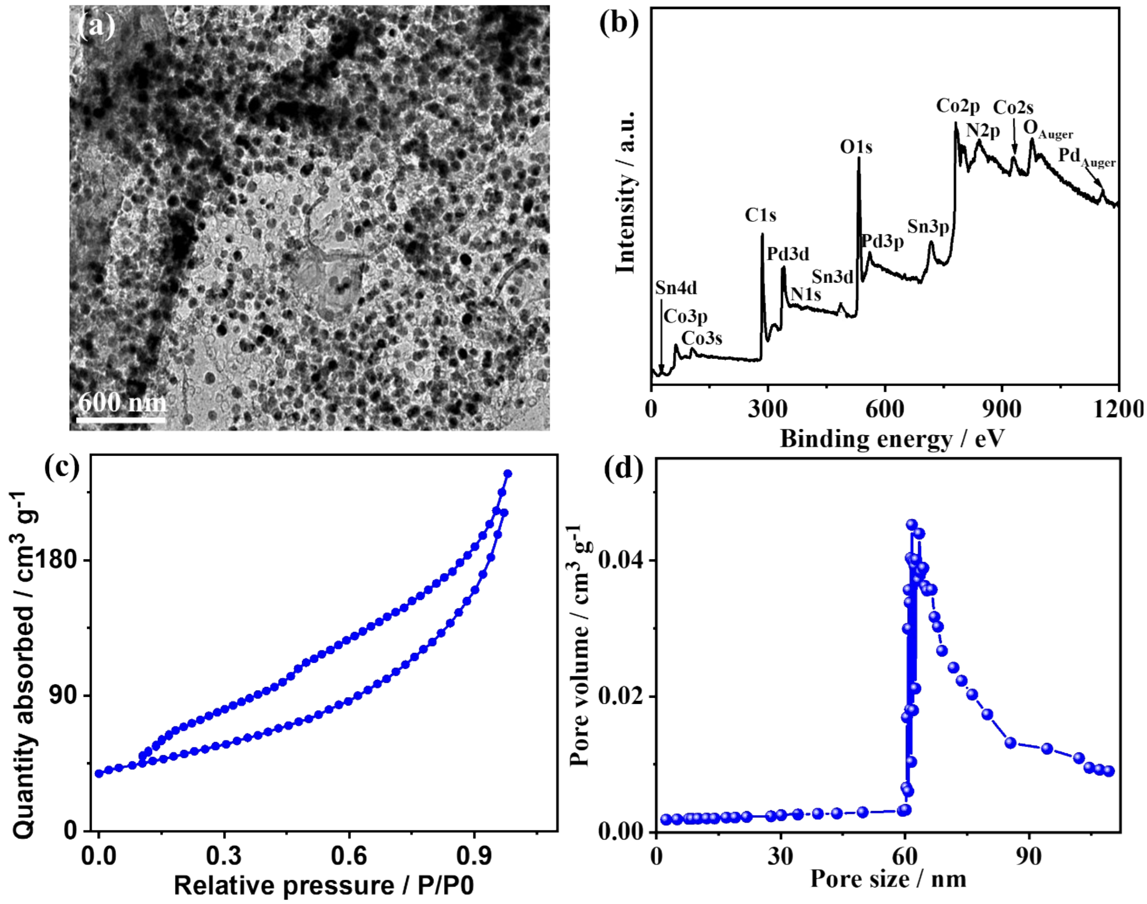

Fig. S6. High-resolution XPS (a) Pd3d and (b) Sn3d, (c) N_2-adsorption/desorption isotherm and (d) pore size distribution of Pd-SnO_2/MOF-PNC after the stability test for 108 h.

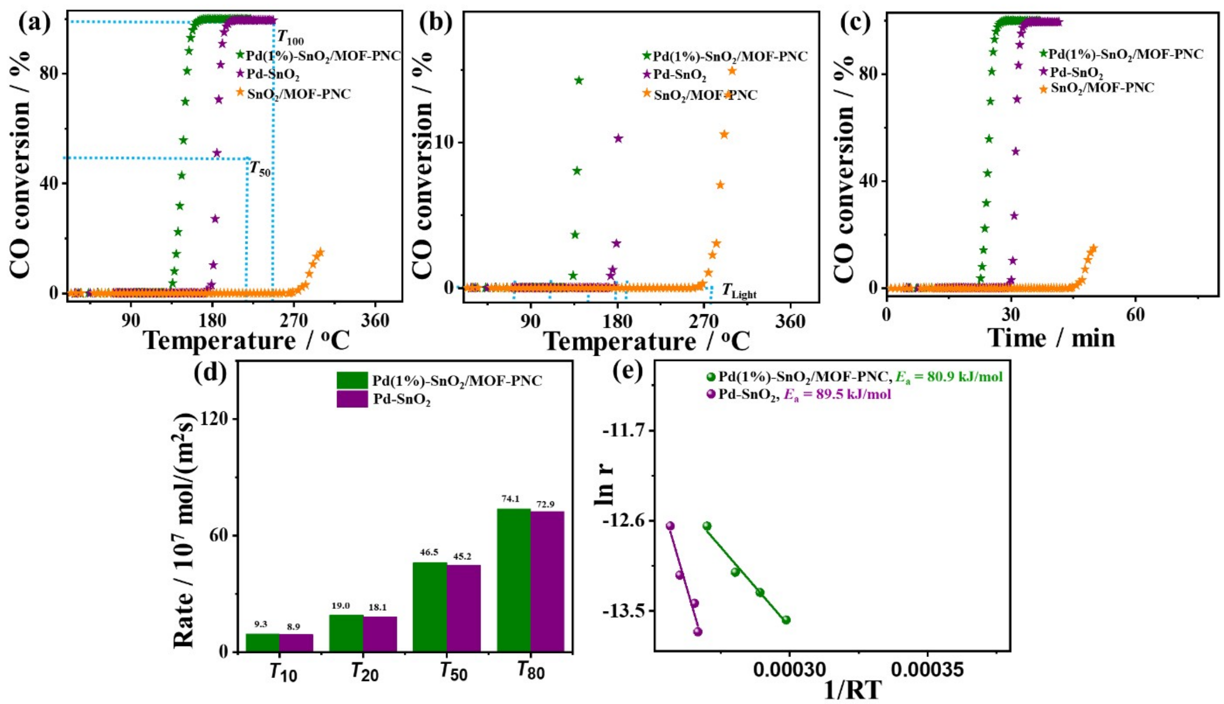

Fig. S7. (a,b) Temperature-dependent CO conversion, (c) Time-dependent CO conversion, (d) Rate at different CO conversion temperatures, and (e) Arrhenius plots of Pd(1%)-SnO_2/MOF-PNC, Pd-SnO_2, and SnO_2/MOF-PNC.

Table S3. Comparative thermal CO oxidation performance of Pd-based catalysts.
MOF-derived porous N-doped carbon (MOF-PNC), high-entropy fluorite oxide (HEFO), hexagonal boron nitride (h-BN), calcination at 500 °C for 18 h (PC3), hydrotalcite-like (HT), SSZ-13 zeolites (SSZ-13), rod-like (R)

Catalysts	Preparation methods	Morphology	T_{100} (°C)	Refs
Pd-SnO_2/MOF-PNC	Microwave-irradiation/annealing/ etching/microwave-irradiation	Spongy-like	65.6	This work
Pd/MOF-PNC	Microwave-irradiation/annealing /etching/microwave-irradiation	Spongy-like	107.9	This work
Pd/CeSn75-800	Counter precipitation/ calcination	Core-shell	~ 100	[1]
Pd@SiO_2/TiO_2-500	Precipitation/ calcination	Core-shell	~ 400	[2]
CeO_2-Pd/S-800-5h	Impregnation/ calcination	2d hexagonal mesopores	~ 75	[3]
Pd_1@HEFO Pd@CeO_2	Ball milling/ annealing/etching	Cubic	170 253	[4]
Pd/MgO(5)-h-BN	Impregnation/ calcination	Nanosheets	140	[5]
$Ce_{1-x}Pd_xO_{2-\delta}$ (PC3)	hydrothermal/reduction/calcination	Nanocrystals	~ 95	[6]
Pd/MgAl-HT	Deposition-precipitation	Nanocrystals	~ 90	[7]
Pd-1%P	Wet-impregnation/ calcination	Fiber-like lamellar	~ 270	[8]

$LaAlPd(0.8)O_3$-600	Impregnation/ Calcination	Perovskite	~ 325	9
$Pd@SiO_2$-673	Polymerization/calcination	Core-shell	~ 130	10
$Pd_{0.83}Co_{0.17}/C$	Wet impregnation	Nanocrystals	150	11
$Pd_{0.5}/CeHfZrSnErO_x$ $Pd_{1.0}/CeHfZrSnErO_x$	Ultrasound-mediated co-precipitation	Cubic	140 150	12
Pd-SSZ-13	Ion exchange/ calcination	Cubic particles	~ 175	13
PdO_x/CeO_2	Radio frequency sputtering	Dendrite-like	250	14
4%Pd/R-CeO_2	Impregnation/ annealing	Rod, cubic, and octahedral	50	15
Pd-Cu/gC_3N_4NWs	Protonation/annealing	Nanowires	149	16
Pd/Cu/gC_3N_4NTs	Protonation/annealing	Nanotubes	154	17
Au/Pd/gC_3N_4NFs	Protonation/annealing	Nanofibers	144	18
Pd- impeded 3D porous graphene (3D Pd-E-PG)	Low-power microwave radiation	3D porous nanosheets	190	19
AuPd/TiO_2	Incipient wetness method	Nanospheres	190	20
Pd/Ni-MOF-HNC Pd/Ni-MOF-NC	Microwave-irradiation/ annealing/etching/microwave-irradiation	Hollow nanosheets	114.5 153.8	21
5wt%Pd/Ce-MOF 7wt%Pd/Ce-MOF 3wt%Pd/Ce-MOF	Hydrothermal/microwave-irradiation	Spherical Pd on needle shaped support	92 148 190	22
2.9%Pd@MIL-101 4.9%Pd@MIL-101 2.2%Pd@MIL-101 1.1%Pd@MIL-101 0.6%Pd@MIL-101 0.3%Pd@MIL-101 0.1%Pd@MIL-101	Hydrothermal/microwave-irradiation	Spherical Ps on nanocubes support	107 147 123 151 151 140 181	23
$Pd_n(1\text{-}Cys)_m/CeO_2$ $Pd_n(1\text{-}Cys)_m/TiO_2$ $Pd_n(1\text{-}Cys)_m/Fe_3O_4$ $Pd_n(1\text{-}Cys)_m/ZnO$	Chemical reduction/impregnation	Monodispersed spherical nanoclusters	110 112 115 155	24

References

1. O. A. Stonkus, A. V. Zadesenets, E. M. Slavinskaya, A. I. Stadnichenko, V. A. Svetlichnyi, Y. V. Shubin, S. V. Korenev and A. I. Boronin, *Catal. Commun.*, 2022, **172**, 106554.
2. A. Takabayashi, F. Kishimoto, H. Tsuchiya, H. Mikami and K. Takanabe, *Nanoscale Adv.*, 2023, **5**, 1124-1132. .
3. P. R. Murthy, S. Munsif, J.-C. Zhang and W.-Z. Li, *Ind. Eng Chem. Res.*, 2021, **60**, 14424-14433.
4. H. Xu, Z. Zhang, J. Liu, C.-L. Do-Thanh, H. Chen, S. Xu, Q. Lin, Y. Jiao, J. Wang and Y. Wang, *Nat. Commun.*, 2020, **11**, 3908.
5. L. Li, X. Liu, H. He, N. Zhang, Z. Liu and G. Zhang, *Catal. Today*, 2019, **332**, 214-221.
6. J. Ye, Y. Xia, D.-g. Cheng, F. Chen and X. Zhan, *Int. J. Hydrog. Energy*, 2019, **44**, 17985-17994.
7. X. Lin, J. Zhou, Y. Fan, Y. Zhan, C. Chen, D. Li and L. Jiang, *Dalton Tran.*, 2018, **47**, 14938-14944.
8. J. Dong, J. Wang, J. Wang, M. Yang, W. Li and M. Shen, *Catal. Sci. Technol.*, 2017, **7**, 5038-5048.
9. Y. J. Kim, J. H. Lim, B. K. Cho, S. B. Hong, I.-S. Nam and J. W. Choung, *J. Catal.*, 2015, **330**, 71-83.
10. Y. Xu, J. Ma, Y. Xu, L. Xu, L. Xu, H. Li and H. Li, *RSC Adv.*, 2013, **3**, 851-858.
11. I. B. Aragão, F. R. Estrada, D. H. Barrett and C. B. Rodella, *Mol. Catal.*, 2022, **526**, 112377.

12. F. Okejiri, J. Fan, Z. Huang, K. M. Siniard, M. Chi, F. Polo-Garzon, Z. Yang and S. Dai, *Iscience*, 2022, **25**, 104214.
13. D. Chen, H. Lei, W. Xiong, Y. Li, X. Ji, J.-Y. Yang, B. Peng, M. Fu, P. Chen and D. Ye, *ACS Catal.*, 2021, **11**, 13891-13901.
14. L. S. Kibis, A. A. Simanenko, A. I. Stadnichenko, V. I. Zaikovskii and A. I. Boronin, *J. Phys. Chem. C*, 2021, **125**, 20845-20854.
15. X. Zhang, W. Li, Z. Zhou, K. Chen, M. Wu and L. Yuan, *Mol. Catal.*, 2021, **508**, 111580.
16. K. Eid, Y. H. Ahmad, A. T. Mohamed, A. G. Elsafy and S. Y. Al-Qaradawi, *Catalysts*, 2018, **8**, 411.
17. K. Eid, M. H. Sliem, K. Jlassi, A. S. Eldesoky, G. G. Abdo, S. Y. Al-Qaradawi, M. A. Sharaf, A. M. Abdullah and A. A. Elzatahry, *Inorg. Chem. Commun.*, 2019, **107**, 107460.
18. K. Eid, M. H. Sliem, A. S. Eldesoky, H. Al-Kandari and A. M. Abdullah, *Int. J. Hydrog. Energy*, 2019, **44**, 17943-17953.
19. R. Kumar, J.-H. Oh, H.-J. Kim, J.-H. Jung, C.-H. Jung, W. G. Hong, H.-J. Kim, J.-Y. Park and I.-K. Oh, *ACS Nano*, 2015, **9**, 7343-7351.
20. A. Teixeira-Neto, R. Gonçalves, C. Rodella, L. Rossi and E. Teixeira-Neto, *Catal. Sci. Technol.*, 2017, **7**, 1679-1689.
21. A. K. Ipadeola, A. Gamal, A. M. Abdullah, A. B. Haruna, K. I. Ozoemena and K. Eid, *Catal. Sci. Technol.*, 2023, **13**, 4873-4882. .
22. A. Lin, A. A. Ibrahim, P. Arab, H. M. El-Kaderi and M. S. El-Shall, *ACS Appl. Mater. Interfaces*, 2017, **9**, 17961-17968.
23. M. S. El-Shall, V. Abdelsayed, S. K. Abd El Rahman, H. M. Hassan, H. M. El-Kaderi and T. E. Reich, *J. Mater. Chem.*, 2009, **19**, 7625-7631.
24. M. Farrag, M. K. Das, M. Moody and M. Samy El-Shall, *ChemPhysChem*, 2021, **22**, 312-322.